JOURNAL OF GUIDANCE, CONTROL, AND DYNAMICS
Vol. 21, No. 1, January–February 1998

Rapid Reorientation Maneuvers of Experimental Spacecraft with a Pendulum Appendage

Feiyue Li* and Peter M. Bainum†
Howard University, Washington, D.C. 20059
and
N. Glenn Creamer‡ and Shalom Fisher§
U.S. Naval Research Laboratory, Washington, D.C. 20375

Recent numerical and experimental results are reported for the near-minimum-time maneuvers of the U.S. Naval Research Laboratory's Reconfigurable Spacecraft Host for Attitude and Pointing Experiments (RESHAPE) facility with a pendulum appendage, which is a three-dimensional, freely rotating platform supported by a spherical air bearing system and equipped with a certain payload, reaction wheels, rate gyros, and an onboard computer. The pendulum appendage is attached vertically by a string to the edge of the RESHAPE's circular platform. The maneuver control uses the summation of an open-loop feedforward command and a feedback command. The feedforward part is obtained from the solution of the time-optimal control of a simplified system. The feedback control, used to damp out small disturbances during the maneuver and postmaneuver errors, is a proportional control formed by feeding back the error between the feedforward command and the measurements. Maneuver simulations and tests show the advantage of using the flexible modeling in the control design. Some interesting phenomena, such as the change of the number of inner switching points and the trajectory feedforward effect, are also presented and discussed. Numerical and experimental results are presented to illustrate the success of the three-dimensional RESHAPE maneuvers and the excellent correlation between the simulations and tests.

Introduction

THE theoretical study of three-dimensional, large-angle attitude maneuvers of spacecraft/satellites with flexible appendages has been the subject of many research papers. However, experimental testing in this area has been limited. This paper focuses on the testing. The majority of published experimental test papers can be considered as two-dimensional tests. Some preliminary three-dimensional test results have been published recently. In a recent paper, the application of near-optimal open-loop and Lyapunov closed-loop control methods to maneuver the ground-based U.S. Air Force Phillips Laboratory Advanced Space Structure Technology Research Experiment (ASTREX) is discussed.[1] The mathematical model accounts for thruster dynamics, fuel constraints, leakage, and multibody interactions and is based on the rigidized ASTREX model. Torque smoothing was used to minimize the high-frequency structural excitations. Some successful tests of three-axis, near-minimum-time maneuvers using the U.S. Naval Laboratory's Reconfigurable Spacecraft Host for Attitude and Pointing Experiments (RESHAPE) facility have been reported in Refs. 2 and 3. These results were based on a rigidized model of the RESHAPE platform representative of three-axis maneuvers of a rigid spacecraft system. In Ref. 2, a feedforward and state-error feedback control strategy was applied. In Ref. 3, a different feedback control based on bang-bang switching functions was employed. In both cases, the experiments corresponded excellently with the numerical simulations.

One of the active research areas in the minimum-time and near-minimum-time maneuvers of flexible spacecraft is in the command shaping technology. To name a few, in Ref. 4, an open-loop, sub-time-optimal computing algorithm based on the parameter optimization technique with robustness considerations was applied to the system with one rigid-body mode and one flexible mode. With the sacrifice in the maneuver time, the addition of more switches to the control profile can increase the robustness and reduce the residual vibration. In Ref. 5, the advantages of using a time-delay filter and Lyapunov controller have been demonstrated to reduce the flexible vibration in general maneuvers and near-minimum-time maneuvers. In Ref. 6, an extensive study of the procedure for designing input shapers was presented. The resulting command has the advantage in robustness, fuel efficiency, and elimination of multiple modes. In contrast to this, in our current paper the focus is not on the input shaping. Instead, the open-loop inputs are obtained by solving the time-optimal maneuver problem with the flexible mode included in the formulation. Therefore, the switching times are determined numerically as long as the system model, system parameters, and maneuver initial and final conditions are chosen.

In this paper, the three-axis maneuver tests of the RESHAPE are extended to include a flexible appendage. The appendage is represented by a pendulum attached vertically by a string to the edge of the RESHAPE's platform (Fig. 1). This attachment increases the order of the system by two dynamic degrees of freedom (DOF). The first DOF of the pendulum can be characterized by the swing angle of the pendulum with respect to the vertical line through the hinge point inside the tangential plane, which could represent a flexible mode under certain conditions. The second DOF is represented by the out-of-the-tangential-plane angular motion. In an analogy to the motion of a flexible structural beam under the restoring force due to elasticity, the motion of the pendulum can be considered as under the influence of the restoring force due to the gravity. Because of the increase of the system order and nonlinear coupling, the attachment of the pendulum introduces challenges to the control system design.

The objective of these maneuver tests is to achieve near-minimum-time maneuvers of the RESHAPE from the known initial states to the final required attitude and, at the same time, to keep the vibration of the pendulum to a minimum amplitude. Initially, the main test interest was focused on the maneuvers about the yaw axis, while the motion about the roll and the pitch axes was kept small. Because the vibration of the pendulum is not expected to be large, small-amplitude vibration modeling can be used in the control design and numerical simulations. As a result, the maneuver

Presented as Paper 96-3622 at the AIAA/AAS Astrodynamics Specialist Conference, San Diego, CA, July 29–31, 1996; received Sept. 10, 1996; revision received June 20, 1997; accepted for publication June 20, 1997.

*Research Associate, Department of Mechanical Engineering. Member AIAA.
†Distinguished Professor of Aerospace Engineering, Department of Mechanical Engineering. Fellow AIAA.
‡Aerospace Engineer, Control Systems Branch. Senior Member AIAA.
§Research Physicist, Systems Analysis Branch. Senior Member AIAA.

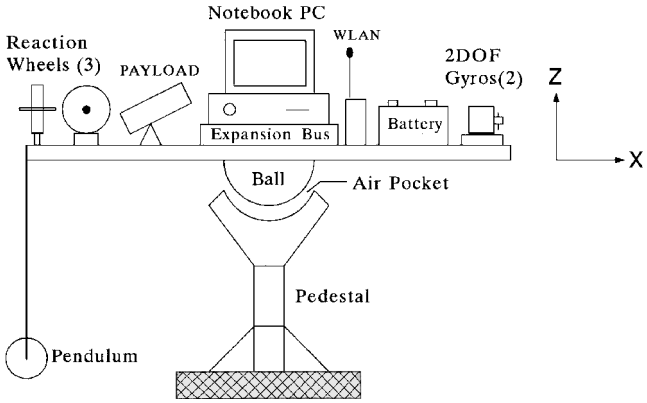

Fig. 1 RESHAPE configuration.

considered here is a confined three-dimensional maneuver because the soft constraints have been imposed by the control strategy.

System Equations

A sketch of the RESHAPE's coordinate system is shown in Figs. 2a and 2b. The body axes are denoted by $(\boldsymbol{i}, \boldsymbol{j}, \boldsymbol{k})$ with origin at o, the pivot point about which the platform can rotate freely. $\boldsymbol{R}$ is a body fixed vector from o to a, the hinge point of the pendulum string to the platform. $\boldsymbol{L}$ is the vector from a to the pendulum, and α is the angle between the string and the vertical line through the hinge point, which represents the first DOF of the pendulum. Shown in Fig. 2b is another set of body axes $(\boldsymbol{i}_m, \boldsymbol{j}_m, \boldsymbol{k}_m)$ with origin at a, where $\boldsymbol{k}_m$ is parallel to $\boldsymbol{k}$ and $\boldsymbol{j}_m$ is parallel to the tangent line at a. Here, β, representing the second DOF, is the angle between the projection line of the pendulum string in the $(\boldsymbol{i}, \boldsymbol{j})$ plane and $\boldsymbol{j}_m$, and β_m is the angle between $\boldsymbol{i}$ and $\boldsymbol{i}_m$. For convenience, the column matrix format representations R and L for the vectors $\boldsymbol{R}$ and $\boldsymbol{L}$ (same for other vectors) will be used throughout the equation development, as defined in the following:

$$\boldsymbol{R} = R_x\boldsymbol{i} + R_y\boldsymbol{j} + R_z\boldsymbol{k}, \qquad \boldsymbol{L} = L_x\boldsymbol{i} + L_y\boldsymbol{j} + L_z\boldsymbol{k}$$

$$R^\top = [R_x \quad R_y \quad R_z], \qquad R_1 = \left(R_x^2 + R_y^2\right)^{\frac{1}{2}}$$

$$R_x = R_1\cos\beta_m, \qquad R_y = R_1\sin\beta_m$$

$$L^\top = L_1[\sin\alpha\sin\bar{\beta} \quad \sin\alpha\cos\bar{\beta} \quad -\cos\alpha], \qquad \bar{\beta} = \beta - \beta_m$$

where R_1 is the magnitude of $\boldsymbol{R}$ projected onto the $(\boldsymbol{i}, \boldsymbol{j})$ plane and L_1 is the length of the pendulum string.

The three-dimensional dynamical equations of motion can be derived using Lagrange's approach. The kinetic energy of the system can be expressed as

$$T = T_M + T_h + T_m$$

where the subscripts M, h, and m refer to the platform, the reaction wheels, and the pendulum, respectively. Then,

$$T_M = \tfrac{1}{2}\omega^\top J_M\omega$$

where ω is the angular velocity vector and J_M is the inertia matrix of the platform about the pivot point o. Both ω and J_M are expressed in body axes $(\boldsymbol{i}, \boldsymbol{j}, \boldsymbol{k})$. Next, by assuming that the rotation axes of the three reaction wheels are aligned orthogonally along the three body axes $(\boldsymbol{i}, \boldsymbol{j}, \boldsymbol{k})$, respectively, one can obtain

$$T_h = \frac{1}{2}\sum_i \omega^\top J_{h_i}\omega + \frac{1}{2}\sum_i J_i\Omega_i^2 + \sum_i J_i\Omega_i\omega_i \qquad i = 1, 2, 3$$

where J_{h_i} is the inertia matrix of the ith wheel with respect to the pivot point, J_i is the moment of inertia of the ith wheel about its rotation axis, and Ω_i is the relative angular rate of the ith wheel with respect to the platform. The kinetic energy related to the pendulum can be obtained as

$$T_m = \tfrac{1}{2}m\left[\dot{L}^\top\dot{L} + 2\omega^\top(\tilde{R} + \tilde{L})\dot{L} + (1/m)\omega^\top J_m\omega\right]$$

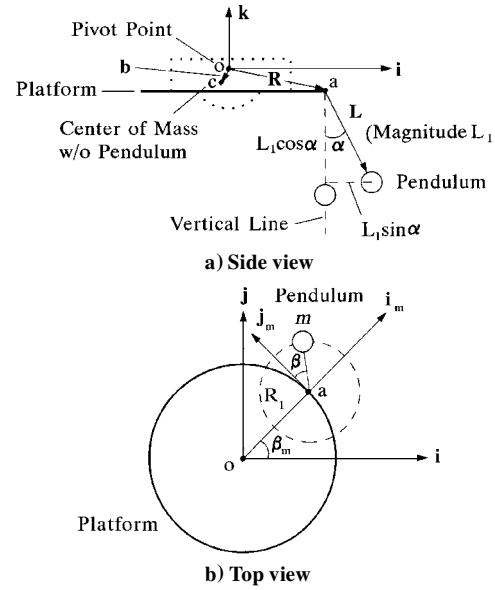

Fig. 2 RESHAPE coordinate system.

where m is the pendulum mass, J_m is the inertia matrix of the pendulum with respect to o, and $\tilde{v}$ is a 3×3 skew-symmetric matrix associated with a vector, $v^\top = [v_1 \quad v_2 \quad v_3]$, where $v_{12} = -v_{21} = -v_3$, etc. The virtual work related to the gravity can be obtained as

$$\delta W_g = -g\left\{\delta\theta^\top[M\tilde{b} + m(\tilde{R} + \tilde{L})] - m\left(\delta\alpha L_\alpha^\top + \delta\beta L_\beta^\top\right)\right\}a_3 \quad (1)$$

where M is the mass of the platform and the three wheels, b is the position vector from the pivot point to the center of mass of the system without the pendulum, g is the gravitational acceleration constant, $\delta\theta$ is the virtual angle displacement vector, q is the attitude quaternion vector $q^\top = [q_0 \quad q_1 \quad q_2 \quad q_3]$, and $a_3^\top = [a_{13} \quad a_{23} \quad a_{33}]$ is the third column of the direction cosine matrix of the platform:

$$a_3^\top = \left[2(q_1q_3 - q_0q_2) \quad 2(q_2q_3 + q_0q_1) \quad 2\left(q_0^2 + q_3^2\right) - 1\right]$$

Using Lagrange's equations for the quasicoordinates (ω_i, $i = 1, 2, 3$, are the time derivatives of the quasicoordinates) for the platform and using the regular Lagrange's equations for the rotation angles φ of the reaction wheels, we can obtain

$$(J_{M+h} + J_m)\dot{\omega} + J_d\dot{\Omega} + m(\tilde{R} + \tilde{L})\ddot{L} = \tilde{\omega}\frac{\partial T}{\partial\omega} - m\dot{\tilde{L}}\dot{L} - \dot{J}_m\omega + Q_\theta \quad (2)$$

$$J_d\dot{\Omega} + J_d\dot{\omega} = \tau_\varphi = -u \quad (3)$$

where $J_d = \text{diagonal}[J_1, J_2, J_3]$, τ_φ is the torque acting on the reaction wheels, J_{M+h} is the inertia matrix of the platform and the wheels together, and Q_θ is the generalized force vector, which can be obtained from Eq. (1). Note that $\dot{R} = 0$ is used here because R is a constant matrix in the body axes. By substituting $\dot{\Omega}$ in Eq. (3) into Eq. (2), we can obtain

$$(J_{M+h} + J_m - J_d)\dot{\omega} + m(\tilde{R} + \tilde{L})\ddot{L} = u + \tilde{\omega}\frac{\partial T}{\partial\omega} - m\dot{\tilde{L}}\dot{L} - \dot{J}_m\omega - g[M\tilde{b} + m(\tilde{R} + \tilde{L})]a_3 \quad (4)$$

At the same time, we can obtain the Lagrange's equations for α and β,

$$m\left[\ddot{L}^\top L_\alpha - L_\alpha^\top(\tilde{R}+\tilde{L})\dot{\omega} - 2L_\alpha^\top\dot{\tilde{L}}\omega - \frac{\omega^\top}{m}\frac{\partial J_m}{\partial\alpha}\omega\right] = -mga_3^\top L_\alpha \quad (5)$$

$$m\left[\ddot{L}^\top L_\beta - L_\beta^\top(\tilde{R}+\tilde{L})\dot{\omega} - 2L_\beta^\top\dot{\tilde{L}}\omega - \frac{\omega^\top}{m}\frac{\partial J_m}{\partial\beta}\omega\right] = -mga_3^\top L_\beta \quad (6)$$

where

$$L_\alpha^\top = \frac{\partial L^\top}{\partial \alpha} = L_1[\cos\alpha \sin\bar{\beta} \quad \cos\alpha\cos\bar{\beta} \quad \sin\alpha]$$

$$L_\beta^\top = \frac{\partial L^\top}{\partial \beta} = L_1 \sin\alpha[\cos\bar{\beta} \quad -\sin\bar{\beta} \quad 0]$$

It can be proven that

$$\ddot{L} = \ddot{\alpha}L_\alpha + \dot{\beta}L_\beta + \left(-\dot{\alpha}^2 L + 2\dot{\alpha}\dot{\beta}L_{\alpha\beta} + \dot{\beta}^2 L_{\beta\beta}\right)$$

where

$$L_{\alpha\beta} = \frac{\partial L_\alpha}{\partial \beta}, \qquad L_{\beta\beta} = \frac{\partial L_\beta}{\partial \beta}$$

After substituting $\ddot{L}$ into Eq. (4), we can see that the coefficient of $\ddot{\beta}$ contains $\sin\alpha$ (see L_β). Therefore, for small α, the out-of-plane motion β has a weak direct contribution to the ω motion. At the same time, $\ddot{\beta}$ does not appear in Eq. (5) because $L_\beta^\top L_\alpha = 0$. To obtain an equivalent single flexible mode model, we have excluded the β motion from further consideration in the following analysis. However, we acknowledge that, for further analysis of the system, the nonlinear effect of the β coupling needs to be considered because $\dot{\beta}$ and β do appear in other parts of these equations. As mentioned earlier, the current interest is mainly in the large-angle maneuvers about the yaw axis. This simplifies the maneuver problem to a single-axis (yaw axis) maneuver of the rigid RESHAPE platform with a pendulum of a single flexible mode (in-plane angular motion). Because the resulting single-axis maneuver is constrained by the control program, not by hard constraints, it is a confined three-dimensional maneuver. Now, these equations can be further simplified for small α and β:

$$\cos\alpha \simeq 1, \qquad \cos\bar{\beta} = \cos(\beta - \beta_m) \simeq \cos\beta_m$$

$$\sin\alpha \simeq \alpha, \qquad \sin\bar{\beta} = \sin(\beta - \beta_m) \simeq -\sin\beta_m$$

In addition, by assuming that q_1, q_2, ω_1, and ω_2 are small and only their linear terms are retained, Eqs. (4) and (5) can be linearized as

$$J_T\dot{\omega} + m[lc \quad ls \quad L_1R_1]^\top\ddot{\alpha}$$

$$= u + \omega_3 \begin{bmatrix} -J_{12}\omega_1 + (J_{33} - J_{22})\omega_2 + J_{23}\omega_3 \\ (J_{11} - J_{33})\omega_1 + J_{12}\omega_2 + J_{13}\omega_3 \\ J_{23}\omega_1 - J_{13}\omega_2 \end{bmatrix} + \tilde{\omega}J_d\Omega$$

$$- Mg \begin{bmatrix} b_2 - b_3a_{23} \\ b_3a_{13} - b_1 \\ b_1a_{23} - b_2a_{13} \end{bmatrix} - mg \begin{bmatrix} R_y + \alpha c + la_{23} \\ -la_{13} - R_x + \alpha s \\ R_xa_{23} - R_ya_{13} \end{bmatrix} \tag{7}$$

$$mL_1^2\ddot{\alpha} + m[lc \quad ls \quad L_1R_1]\dot{\omega} = 2m\omega_3 l(c\omega_2 - s\omega_1)$$

$$- mg[ca_{23} - sa_{13} + L_1\alpha] \tag{8}$$

Note that these are linear equations for α, β, q_1, q_2, ω_1, and ω_2 only. J_{ij} is the element of the constant inertia matrix J_T, where

$$J_T = J_{M+h} + \bar{J}_m - J_d, \bar{J}_m = m \begin{bmatrix} R_y^2 + l^2 & -R_xR_y & R_xl \\ -R_xR_y & R_x^2 + l^2 & R_yl \\ R_xl & R_yl & R_1^2 \end{bmatrix}$$

$$l = L_1 - R_z, \qquad c = L_1\cos\beta_m, \qquad s = L_1\sin\beta_m$$

These equations will be used in the three-dimensional numerical simulations. To further simplify the analysis, we can neglect the terms related to the gravity, the body rates, and the rates of the wheels in the ω equation and the terms related to the body rates and quaternions in the α equation:

$$J_T\dot{\omega} + m[lc \quad ls \quad L_1R_1]^\top\ddot{\alpha} = u \tag{9}$$

$$mL_1^2\ddot{\alpha} + m[lc \quad ls \quad L_1R_1]\dot{\omega} = -mgL_1\alpha \tag{10}$$

The equations for a system with two DOF involving only ω_3 and α can be obtained as

$$\left(J_{(M+h)_3} - J_{h_3} + mR_1^2\right)\dot{\omega}_3 + mL_1R_1\ddot{\alpha} = u_3 \tag{11}$$

$$mR_1L_1\dot{\omega}_3 + mL_1^2\ddot{\alpha} = -mgL_1\alpha \tag{12}$$

Feedforward and Feedback Controls

The two-DOF linear equations (11) and (12) are used for the control system design. The time-optimal control for the two-DOF system can be obtained by using the maximum principle. The formulation of the time-optimal control is based on the following cost functional:

$$J = \int_0^{t_f} \mathrm{d}t = t_f$$

with constraint equations $|u_i| \le u_{i\max}$ and the following boundary conditions of the state variables associated with rest-to-rest maneuvers:

$t = 0$:

$$\alpha(0) = 0, \qquad \dot{\alpha}(0) = 0, \qquad \theta_3(0) = \theta_{30}, \qquad \omega_3(0) = 0$$

$t = t_f$:

$$\alpha(t_f) = 0, \qquad \dot{\alpha}(t_f) = 0, \qquad \theta_3(t_f) = 0, \qquad \omega_3(t_f) = 0$$

The Hamiltonian of the system can be formed by introducing costates, and the necessary conditions can be derived. The control is of the bang-bang type and can be obtained numerically by solving the associated two-point boundary-value problem using a shooting method.[2]

Once the two-DOF solution is obtained, it is expanded to the three-dimensional solution by adding zero time histories for the augmented variables associated with the three-dimensional system. The resulting three-dimensional solution, including the time history of the quaternions $q(t)$, the angular velocities $\omega(t)$, and the control torques $u(t)$, is used as the open-loop control or feedforward commands of the three-dimensional system. The solution for $\alpha(t)$ is not considered in the feedback control loop because there are no direct measurements for it. During the test, the differences between these computed commands and the real-time measurements of these variables are

$$dq = q_m - q(t), \qquad d\omega = \omega_m - \omega(t)$$

where ω_m is obtained from the output of the rate gyros and q_m is obtained from integration of the kinematic equations using Euler's first-order integration method. To correct the cumulated numerical error, in both the test and the numerical simulation, the constraint between the quaternions (q_0–q_3) is enforced by dividing the square root of the sum of the square of them at each sampling time interval or integration step. The error quaternion dq and the error angular velocity $d\omega$ are used in the state-error feedback control loop to obtain the correction control du

$$du_i = -k_p dq_i - k_r d\omega_i, \qquad i = 1, 2, 3$$

where k_p and k_r are constants. The resulting total control signal is the summation of the open-loop control and the feedback control:

$$u(t, dq, d\omega) = u(t) + du$$

It is clear that the torque constraints for the open-loop bang-bang control should be set below the maximum allowable level $u_{i\max}$

of the physical system, so that some leeway can be left for the feedback control use. Because the final total control is usually not of the bang-bang type, these maneuvers are called near-minimum-time maneuvers under the allowable control constraints.

Tests and Numerical Simulations

The description of the RESHAPE facility can be found in Refs. 7 and 8. The six elements of the symmetric 3×3 inertial matrix of the RESHAPE without the pendulum, J_{M+h}, $[(\cdot)_{11}, (\cdot)_{22}, (\cdot)_{33}, (\cdot)_{12}, (\cdot)_{13}, (\cdot)_{23}] = [14.42, 17.85, 27.82, 0.15, 0.28, 0.42]$ (ft-lb-s^2). The RESHAPE parameters used in the simulations and tests are listed in Table 1.

Two-DOF Solution and Three-Dimensional Simulation

For the two-DOF system, we have obtained maneuver solutions from $\theta_{30} = 1$ to 180 deg. Two typical maneuvers, 25 and 180 deg, are selected for the three-dimensional simulations [using Eqs. (3), (7), and (8)], and the results are shown in Figs. 3a–3f and 4a–4f, respectively. The dashed lines represent the two-DOF solution, and the solid lines represent the three-dimensional simulations. The minimum time is 11.312 s for the 25-deg case and 30.091 s for the 180-deg case. The quaternions and quaternion errors are shown in Figs. 3a, 4a, 3b, and 4b. The angular velocities are shown in Figs. 3c and 4c. The time-optimal controls (Figs. 3d and 4d) for these maneuvers are of the bang-bang type, and three intermediate switches are required. The occurrence of triple switches is clearly associated with the addition of the flexible mode in the system as compared with the purely single-axis maneuver of a rigid body. The well-known result for the latter case is a single switch in the middle. It is shown that the pendulum angle (Figs. 3e and 4e) and pendulum rate (Figs. 3f and 4f) are very small for this particular RESHAPE system setup. This small-amplitude vibration is also observed during the hardware test. It can be seen that the small differences exist between the three-dimensional simulation and the two-DOF solution for the yaw axis motion represented by the angular rate and control torque. The errors in the motion about the other axes are also very small (Figs. 3b and 4b).

Table 1 RESHAPE parameters

$J_1 = J_2 = J_3$	0.054 ft-lb-s^2
g	32.174 ft/s^2
Mg	638.0 lb
mg	5.0 lb
$b_1 = b_3$	0.0
$u_{3\max}$	0.4 ft-lb
$\mathrm{d}u_3$	$0.001056 \sim 0.08976$ ft-lb
k_p	[24.8846 30.2138 49.7636]
k_r	[44.22 53.69 88.43]
β_m	$\pi/2$
R_1	2.5 ft
R_z	0.0
L_1	4.5 ft
b_2	$-mR_1/M$
$\mathrm{d}u_2 = \mathrm{d}u_1 = 0.5\,\mathrm{d}u_3$	
Sampling time	0.05 s

Interval Between Inner Switches

The three inner switches are separated by approximately 0.568 s for the 25-deg and 0.577 s for the 180-deg maneuvers, as shown in Figs. 3d and 4d, respectively. However, we have observed that the time interval between the triple switches is different from case to case (through computations for the maneuver solutions from $\theta_{30} = 1$ to 180 deg), depending on the system parameters and initial conditions. If all other parameters are fixed and only the initial condition θ_{30} is changed from 1 to 180 deg, the time interval between the three switches changes periodically. At some particular values of θ_{30}, we are able to obtain a zero interval. This means a single-switch case where all of the three switches are collapsed together, even with a flexible mode involved. Except for these isolated points, all other

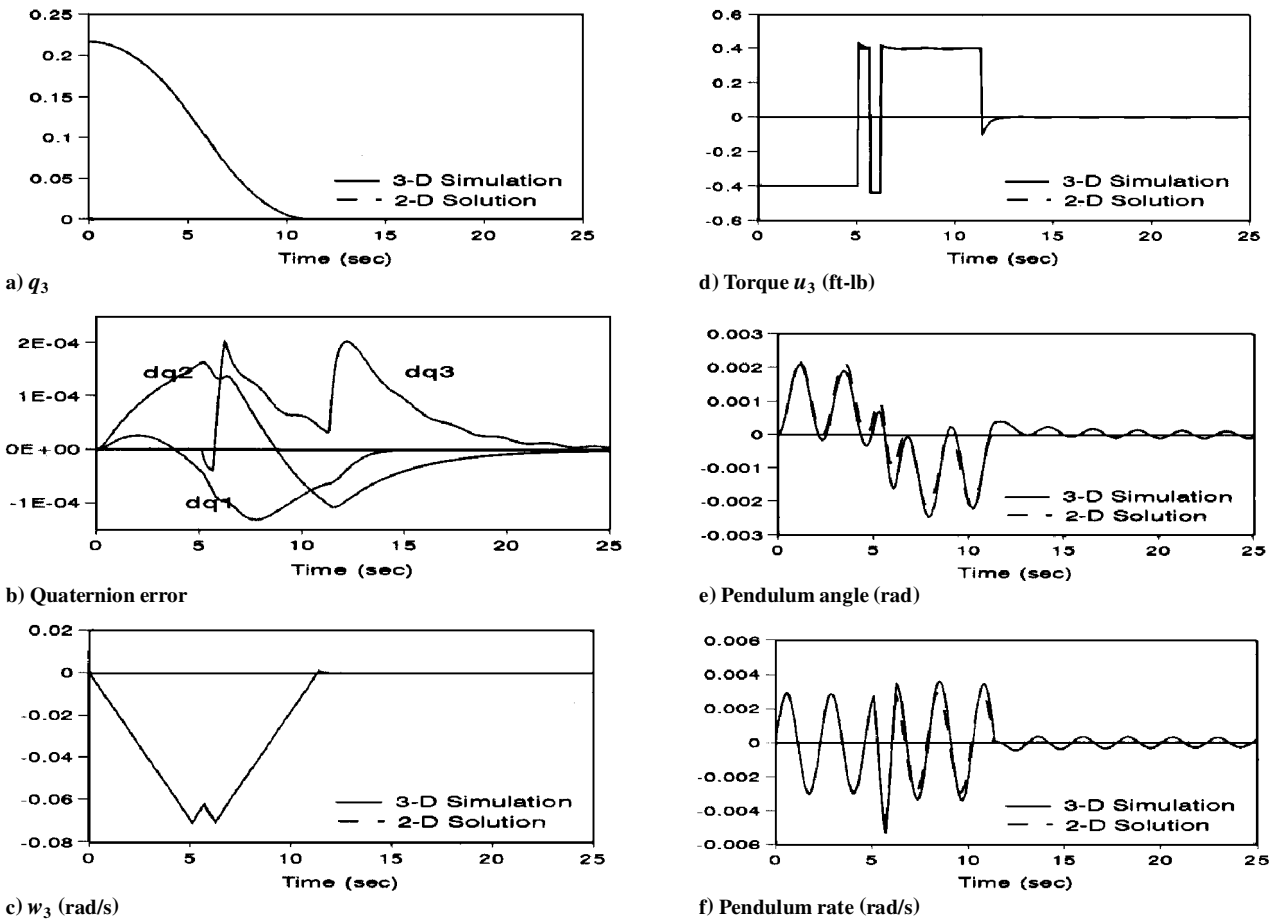

a) q_3 d) Torque u_3 (ft-lb)

b) Quaternion error e) Pendulum angle (rad)

c) w_3 (rad/s) f) Pendulum rate (rad/s)

Fig. 3 Results of 25-deg maneuver, two-DOF solution and three-dimensional simulation.

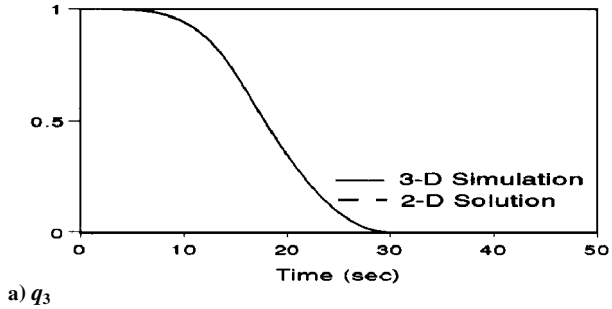

a) q_3

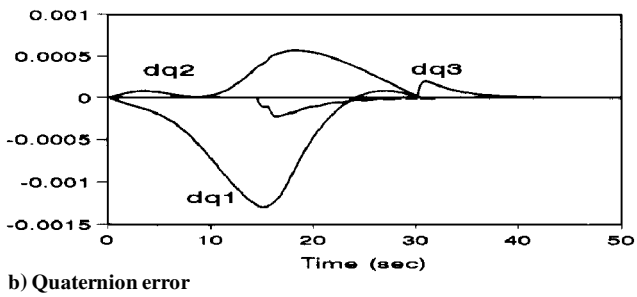

b) Quaternion error

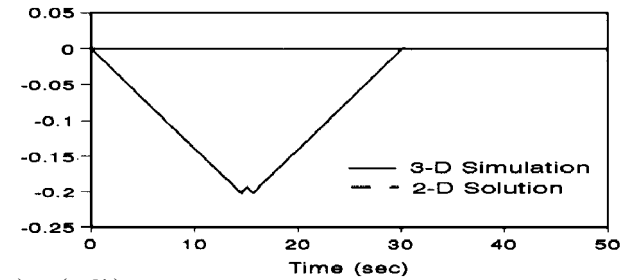

c) w_3 (rad/s)

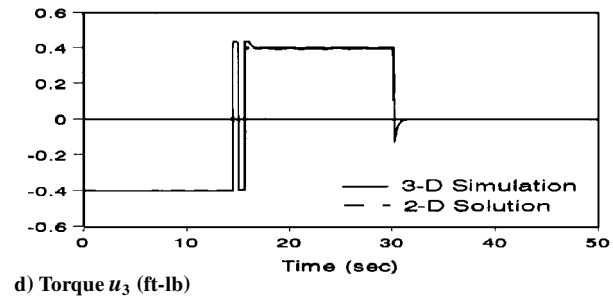

d) Torque u_3 (ft-lb)

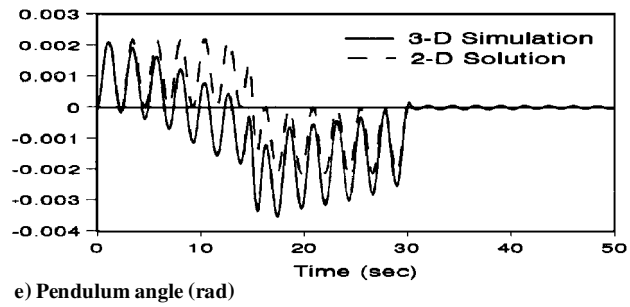

e) Pendulum angle (rad)

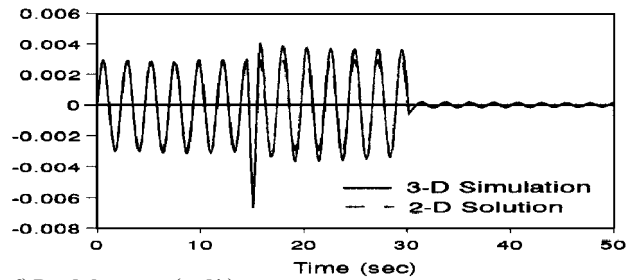

f) Pendulum rate (rad/s)

Fig. 4 Results of 180-deg maneuver, two-DOF solution and three-dimensional simulation.

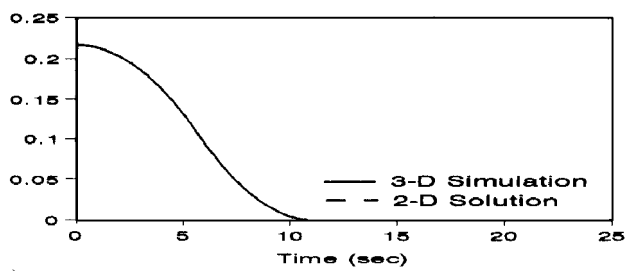

a) q_3

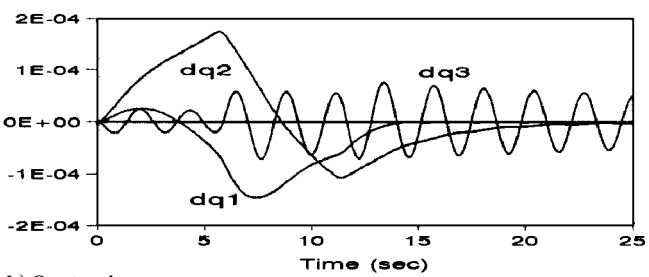

b) Quaternion error

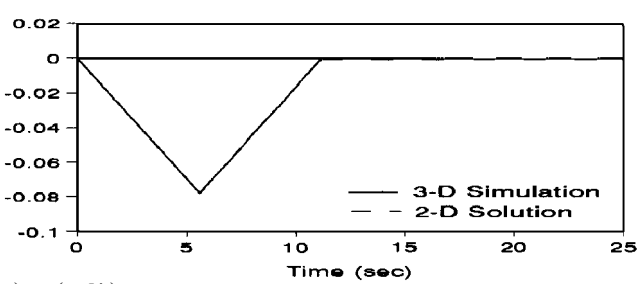

c) w_3 (rad/s)

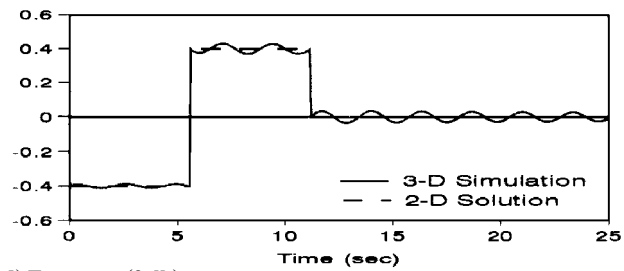

d) Torque u_3 (ft-lb)

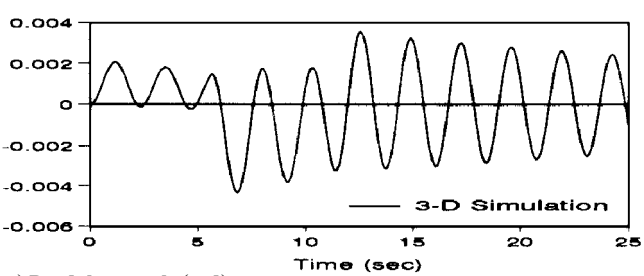

e) Pendulum angle (rad)

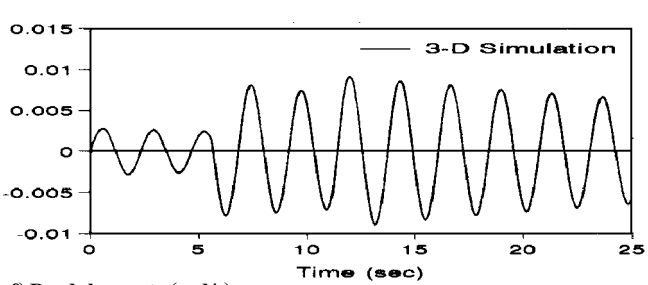

f) Pendulum rate (rad/s)

Fig. 5 Results of 25-deg maneuver, two-DOF solution and three-dimensional simulation, single switch.

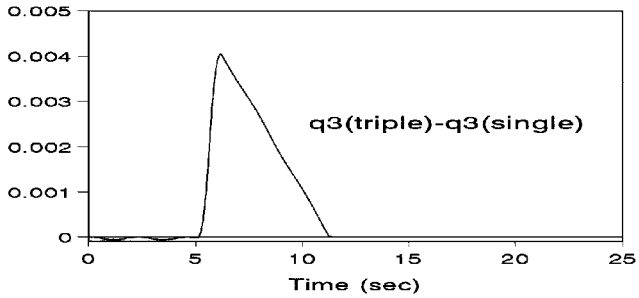

a) dq_3

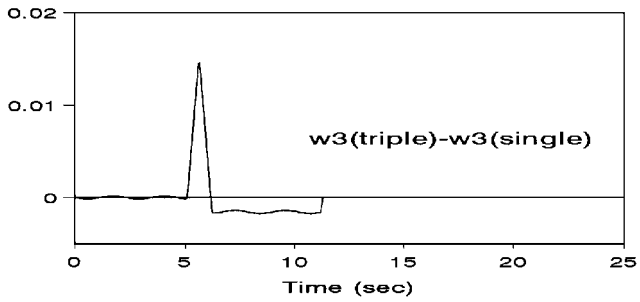

b) dw_3 (rad/s)

Fig. 6 Feedforward trajectory difference between triple- and single-switch cases, 25-deg maneuver.

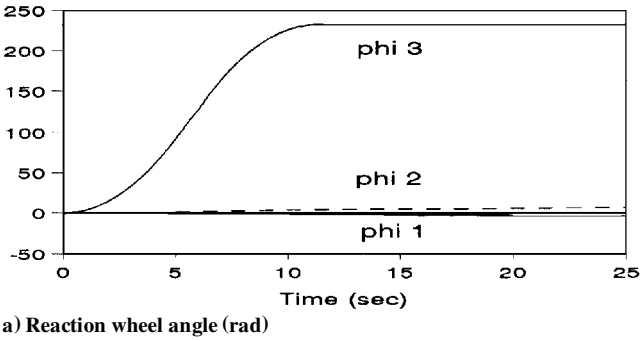

a) Reaction wheel angle (rad)

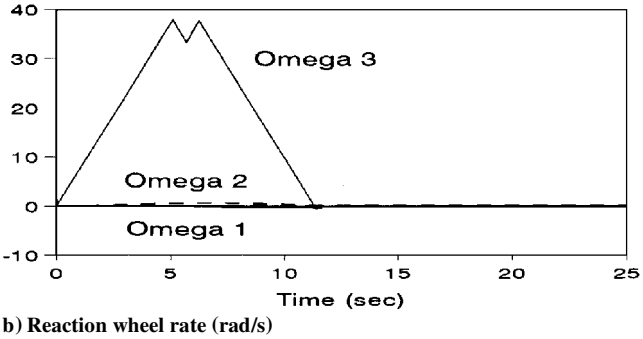

b) Reaction wheel rate (rad/s)

Fig. 7 Reaction wheel responses for the triple-switch case, 25-deg maneuver simulation, du_3 = 0.03696 ft-lb.

cases result in triple switches. It may also be true that changes in other parameters lead to similar results. We choose the 25-deg maneuver because the triple switches in this case are well separated, and we choose the 180-deg case because it can be considered as the largest angle rotation for the rest-to-rest maneuvers.

Triple-Switch vs Single-Switch Solutions

The solution for the time-optimal two-DOF maneuvers is usually not available in analytical form compared with the classical single-axis rigid body maneuver and, therefore, cannot be generated at run time. However, we are interested in finding out the advantage of applying this solution to the maneuver test over using the single-switch solution. Let us now look at results of the three-dimensional simulations for these two open-loop control commands.

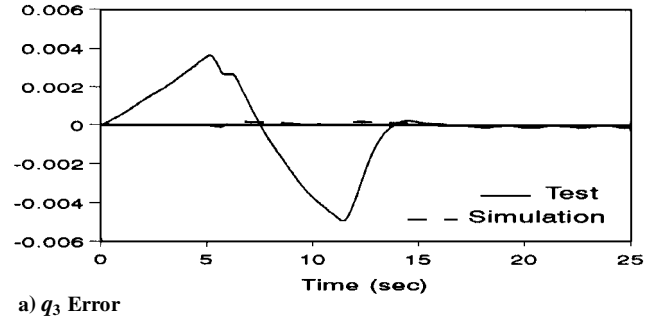

a) q_3 Error

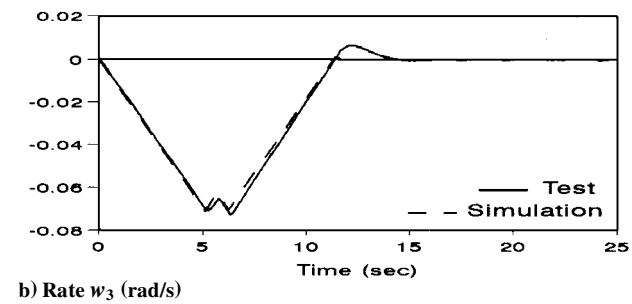

b) Rate w_3 (rad/s)

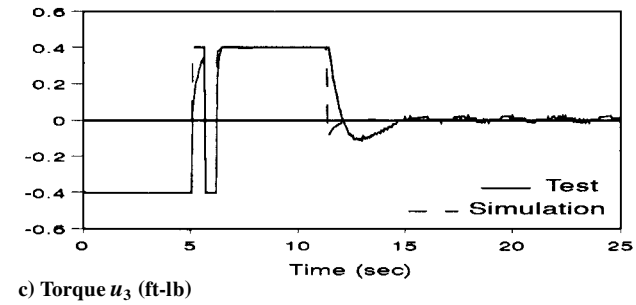

c) Torque u_3 (ft-lb)

Fig. 8 Results of 25-deg maneuver, test and simulation, du_3 = 0.001056 ft-lb.

The simulation results for the single-switch, 25-deg maneuver case are shown in Figs. 5a–5f to compare them with the triple-switch results in Figs. 3a–3f. The single-switch command is obtained from the solution of the simplified one-DOF system as if there is no flexible part. By comparing Figs. 3a–3d with Figs. 5a–5d, the rigid-body responses are basically the same, except that the quaternion error dq_3 vibrates (Fig. 5b). The large differences for these two switch schemes are shown in the pendulum responses (Figs. 3e, 3f, 4e, and 4f). The flexible mode, which has been excited in the single-switch maneuver, is being accounted for in the triple-switch control design. Using the triple-switch command will reduce the vibration of the pendulum both during the second half of the maneuver and postmaneuver. This in return will reduce the attitude errors and rates.

Trajectory Feedforward and Control Feedforward

From the control formulation in the preceding section, we use both control command feedforward and state trajectory feedforward in the test and simulation. This is quite different from the method of using only the control command feedforward. Actually, we can observe the effect of the trajectory feedforward by examining Figs. 3a–3f and 5a–5f. As shown in Figs. 3d and 5d, before the first switch near 5 s, both open-loop control commands are the same, $u_3 = -0.4$ ft-lb. But the three-dimensional responses of the total control u_3 are different. Also the dq_3 in Figs. 3b and 5b are different. This is because the solutions of state $q_3(t)$ from the one-DOF and two-DOF systems are different. The flexible mode is considered in the triple-switch case, whereas it is not in the single-switch case. The differences in q_3 and ω_3 between these two switch schemes are shown in Figs. 6a and 6b, respectively. This can be made more clear if one looks at Eq. (11). It is the α acceleration term that makes a contribution to the solution of the two-DOF system. With the trajectory feedforward, $q(t)$ and $\omega(t)$, the system response can be forced to closely follow the open-loop response.

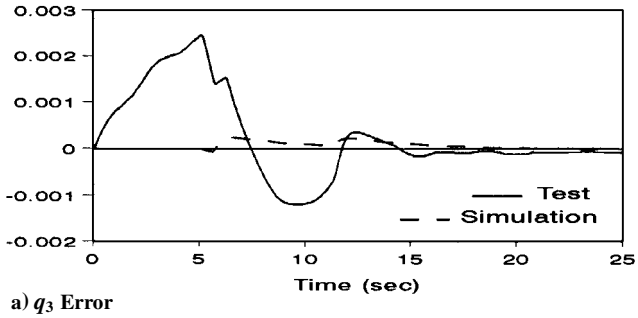

a) q_3 Error

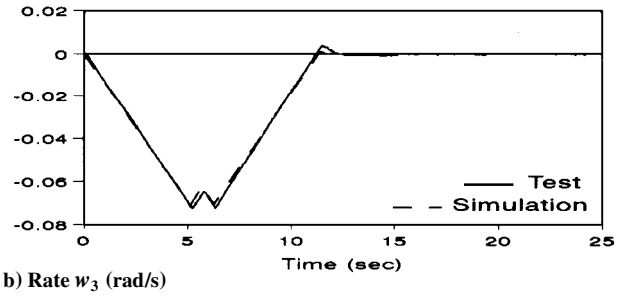

b) Rate w_3 (rad/s)

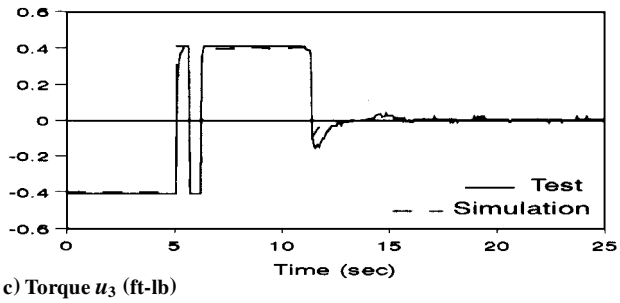

c) Torque u_3 (ft-lb)

Fig. 9 Results of 25-deg maneuver, test and simulation, du_3 = 0.01056 ft-lb.

Reaction Wheel Responses

The time responses of the reaction wheels for the triple-switch simulation, φ and Ω, are shown in Figs. 7a and 7b for the case $du_3 = 0.03696$ (given for information purposes only). The wheel responses for other cases are similar. The nonzero values in Ω are due to the gravitational torque terms presented in Eq. (7). This phenomenon is also observed during the test, where the reaction wheels for the x and y axes keep running after the maneuver. If the values of α or q are not zero, there will be some gravitational torques on the platform, which balance the torques from the reaction wheels. Even though the torques applied to the wheels are zero, other parameters or factors may also lead to the nonzero momentum accumulation of the wheels during the maneuver.

Test and Simulation Results

Using the feedforward and state-error feedback method, we have conducted the hardware tests. Four test results for the 25-deg maneuver using the triple-switch command are presented in Figs. 8–11 for four different levels of the extra control effort du_3 in the feedback control loop: 0.001056, 0.01056, 0.03696, and 0.08976 ft-lb. They are about 0.2–22% of the open-loop control saturation level, 0.4 ft-lb. Also shown in Figs. 8–11 are the three-dimensional simulations using the three-dimensional equations (3), (7), and (8) for comparison purposes. The dashed lines represent the simulation, and the solid lines represent the test results.

As the extra control effort is increased (from Fig. 8c to Fig. 11c), the errors of q_3 (from Fig. 8a to Fig. 11a) are reduced and the overshoot of ω_3 (from Fig. 8b to Fig. 11b) at the end of the maneuver is also reduced. The errors for q_1, q_2, ω_1, and ω_2 are quite small compared with q_3 and ω_3 and are not shown. We also see that the control history of the simulation is close to the open-loop control command (not shown), whereas the control signal from the test deviates more from the open-loop solution for either the smaller leeway case

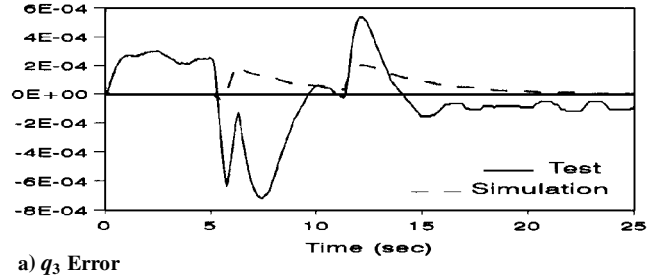

a) q_3 Error

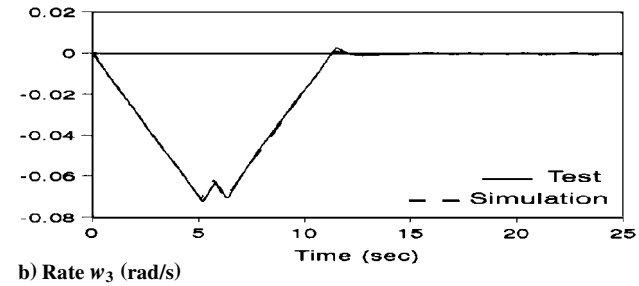

b) Rate w_3 (rad/s)

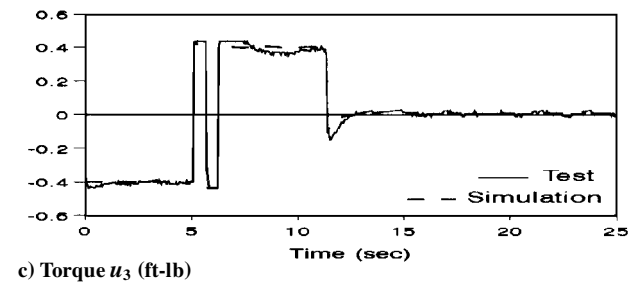

c) Torque u_3 (ft-lb)

Fig. 10 Results of 25-deg maneuver, test and simulation, du_3 = 0.03696 ft-lb.

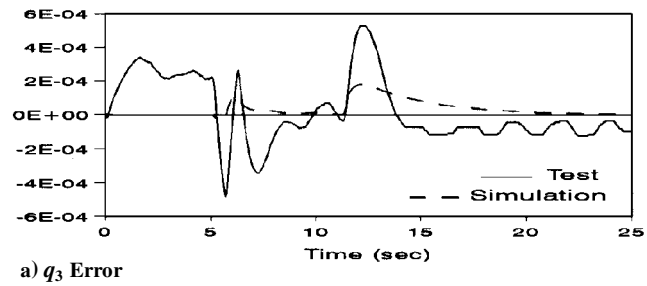

a) q_3 Error

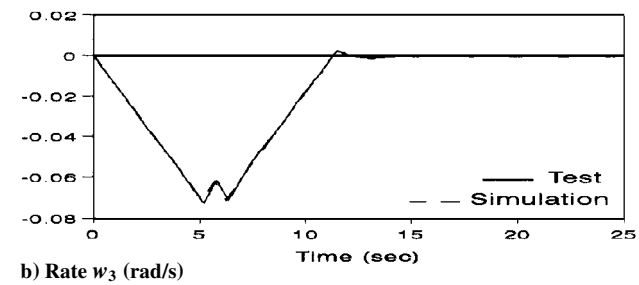

b) Rate w_3 (rad/s)

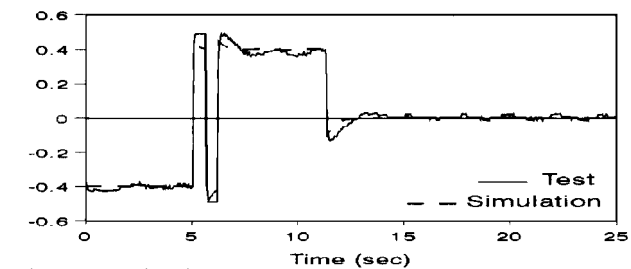

c) Torque u_3 (ft-lb)

Fig. 11 Results of 25-deg maneuver, test and simulation, du_3 = 0.08976 ft-lb.

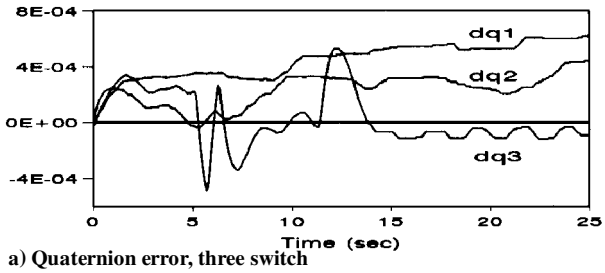

a) Quaternion error, three switch

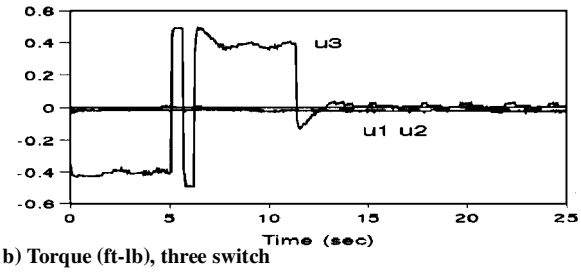

b) Torque (ft-lb), three switch

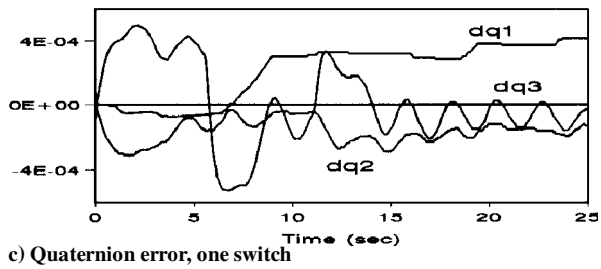

c) Quaternion error, one switch

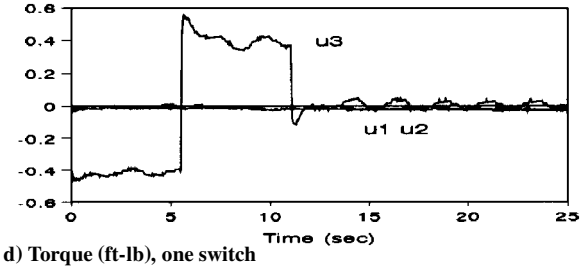

d) Torque (ft-lb), one switch

Fig. 12 Results of 25-deg maneuver tests: triple-switch case, du_3 = 0.08976 ft-lb and single-switch case, $du_3 > 0.08976$ ft-lb.

(Fig. 8c) or the larger leeway case (Fig. 11c). As a rule of thumb, we can use $80 \sim 90\%$ of the allowable control for the open-loop control design and $10 \sim 20\%$ for the correction control. We believe that the overshoot of the control at the end of the maneuver is due to the inaccuracy of the inertial term and the difference in the inertial terms between the two-DOF and three-dimensional representative models of the system.

For the purpose of comparison, the test using the single-switch command was also conducted. Figures 12a and 12b show the triple-switch case, $du_3 = 0.08976$; and Figs. 12c and 12d show one case for the single-switch method, $du_3 > 0.08976$. We observe that the triple-switch method results in less residual vibration, even when the error magnitudes are the same. This indicates the advantage of using the triple-switch solution especially for the well-separated time interval between the three middle switches.

Conclusions

The feedforward and error-state feedback control strategy for the near-minimum-time maneuver problem has been successfully applied to the RESHAPE hardware test facility. The open-loop time-optimal control provides a basis for the nonlinear, large-angle, near-minimum-time maneuver, whereas the linear feedback control takes care of disturbances during the maneuver and damps out the residual vibration after the maneuver. This is the first time that the bang-bang type and feedback control strategy has been applied to the RESHAPE hardware testing facility with flexible appendages. The success of the test is demonstrated by the excellent correlation between numerical simulations and experimental test results. As the extra control effort is increased, the state errors are reduced. An adequate level of the extra control leeway seems to be about 10% of the open-loop control saturation level so that the control will be close to the bang-bang type, the maneuver will be much nearer minimum time, and less postmaneuver vibration and fewer state errors will result. The advantage of using the triple-switch solution over the single-switch solution is indicated in both simulations and tests. Further analysis needs to be done for the reduction of the terminal quaternion and angular rate errors. Improvements and extensions of the control strategy to more bonafide three-axis maneuvers and vibration suppression of the rigid platform containing other types of flexible appendages are recommended.

Acknowledgments

This research was supported by U.S. Air Force Office of Scientific Research Grant F 49620-92-J-0165 and the NASA/Howard University Center for the Study of Terrestrial and Extraterrestrial Atmospheres.

References

[1] Vadali, S. R., Carter, M. T., Singh, T., and Abhyankar, N. S., "Near Minimum Time Maneuvers of Large Structures: Theory and Experiments," *Journal of Guidance, Control, and Dynamics*, Vol. 18, No. 6, 1995, pp. 1380–1385.

[2] Li, F., Bainum, P. M., Creamer, N. G., Fisher, S., and Teneza, N. C., "Three-Axis Near-Minimum-Time Maneuvers of RESHAPE: Numerical and Experimental Results," *Journal of the Astronautical Sciences*, Vol. 43, No. 2, 1995, pp. 161–178; also AAS/AIAA Space Flight Mechanics Meeting, AAS Paper 94-154, Cocoa Beach, FL, Feb. 1994.

[3] Li, F., Bainum, P. M., Creamer, N. G., Fisher, S., and Teneza, N. C., "RESHAPE Experiments for Near-Minimum-Time Feedback Maneuvers," *Proceedings of the 19th International Symposium on Space Technology and Science* (Yokohama, Japan), edited by M. Hinada, AGNE SHOFU, Tokyo, Japan, 1994, pp. 295–301 (Paper 94-C-15).

[4] Liu, Q., and Wie, B., "Robust Time-Optimal Control of Uncertain Flexible Spacecraft," *Journal of Guidance, Control, and Dynamics*, Vol. 15, No. 3, 1992, pp. 597–604.

[5] Singh, T., and Vadali, S. R., "Input-Shaped Control of Three-Dimensional Maneuvers of Flexible Spacecraft," *Journal of Guidance, Control, and Dynamics*, Vol. 16, No. 6, 1993, pp. 1061–1068.

[6] Singhose, W., Derezinski, S., and Singer, N., "Extra-Insensitive Input Shapers for Controlling Flexible Spacecraft," *Journal of Guidance, Control, and Dynamics*, Vol. 19, No. 2, 1996, pp. 385–391.

[7] Creamer, N. G., and Teneza, N. C., "RESHAPE: An Experimental Facility for Satellite Control," *Proceedings of the American Control Conference* (Chicago, IL), 1992, pp. 2001–2005.

[8] "RESHAPE: A Laboratory for Research in Satellite Attitude Control and Control/Structures Interaction," U.S. Naval Research Lab., Rept., Washington, DC, 1992.